Engineering integrated pure narrow-band photon sources

2012 New J. Phys. 14 033008

(http://iopscience.iop.org/1367-2630/14/3/033008)

New Journal of Physics
The open-access journal for physics

Engineering integrated pure narrow-band photon sources

E Pomarico[1,3], B Sanguinetti[1], C I Osorio[1], H Herrmann[2] and R T Thew[1]

[1] Group of Applied Physics, University of Geneva, 1211 Geneva, Switzerland
[2] Angewandte Physik, University of Paderborn, 33095 Paderborn, Germany
E-mail: enrico.pomarico@unige.ch

New Journal of Physics **14** (2012) 033008 (13pp)
Received 8 September 2011
Published 6 March 2012
Online at http://www.njp.org/
doi:10.1088/1367-2630/14/3/033008

Abstract. Engineering and controlling well-defined states of light for quantum information applications is of increasing importance as the complexity of quantum systems grows. For example, in quantum networks, high multi-photon interference visibility requires properly devised pure photon sources. In this paper, we present a theoretical model for a spontaneous parametric down conversion source based on an integrated cavity-waveguide, where single narrow-band, possibly distinct, resonant modes for the idler and the signal fields can be generated. This mode selection takes advantage of the *clustering* effect, due to the intrinsic dispersion of the nonlinear material. We show that, by engineering the clustering effect in an integrated cavity-waveguide and by using a standard detector, one can efficiently generate heralded pure single photons even with a continuous-wave pumping mode. The photon source proposed in this paper is extremely flexible and could easily be adapted to a wide variety of wavelengths and applications, such as long-distance quantum communication.

[3] Author to whom any correspondence should be addressed.

Contents

1. Introduction

Engineering pure quantum states of light is becoming increasingly important for a multitude of applications associated with quantum information technologies, such as the implementation of quantum repeaters [1–3], device-independent quantum key distribution (QKD) [4], entangled states for quantum metrology [5, 6] or for optical quantum computation [7, 8]. This is especially relevant for the scalability of resources in complex quantum systems: for instance, for the realization of a quantum communication network, for which multiple independent systems need to be interfaced with high interference visibility, engineering suitable photon pair sources is crucial.

In recent years, we have seen a concerted effort to develop pure photon sources via spontaneous parametric downconversion (SPDC) or four-wave mixing [9–11]. However, these approaches usually generate relatively broadband photons. Long-distance quantum communication [12, 13], on the other hand, requires narrow-band photons, either for coupling to quantum memories [3] or simply for robustness against thermal dilation of optical fibers [14]. Moreover, we require these sources to be efficient, by which we mean that both the spatial and the spectral modes have to be efficiently selected. The former requires optimal coupling into a single-mode optical fiber, whereas the latter implies spectral purity, which is generally achieved via filtering.

The problem with filtering is that it is inherently lossy: a Gaussian-shaped filter, even if perfectly transparent at its central wavelength, will always introduce some loss in the wings, resulting in the transmission of only $1/\sqrt{2} \approx 70\%$ of the light inside its own spectrum. Emerging applications such as device-independent QKD [4], as well as more fundamental challenges such as all-optical loophole-free Bell tests [15], cannot be realized even with this trivial loss mechanism. Sources compatible with long-distance quantum communication have so far followed two paths: SPDC sources pumped in a continuous-wave (CW) mode and using strong filtering [16, 17], or optical parametric oscillators (OPO) [18–21]. The latter provide quite a

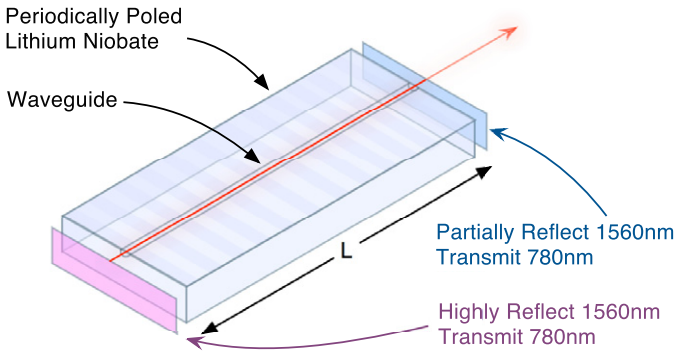

Figure 1. An integrated cavity-waveguide formed by reflection coating mirrors at the entrance and exit surfaces of a periodically poled nonlinear material.

good solution, since they naturally produce narrow-band photons and avoid the Gaussian loss, but are generally complex and require complicated and time-consuming (off-line) stabilization routines.

In this paper, we introduce an integrated OPO approach, which exploits a spectral clustering effect, related to the intrinsic dispersion of the nonlinear crystal and observed in [22], to suppress undesired resonant modes and obviate the need for filtering. Avoiding the use of external filters allows one to increase the rates for long-distance quantum communication experiments. This integrated OPO requires only a simple (and continuous) temperature stabilization. One can obtain a simple, flexible and efficient source of narrow-band heralded pure single photons by detecting one of the down converted photons with a sufficiently fast detector [23, 24]. Such a heralded pure single-photon source can be built up even with a CW pump.

First, we explain the concept of an integrated OPO photon pair source, what the clustering effect is and how it arises from the dispersion of the nonlinear crystal. We then test our theoretical model against some preliminary experimental results and provide easily adaptable guidelines on how to design an integrated cavity-waveguide for a wide variety of wavelengths and applications. An example of such a source is also given. Finally, we discuss the potential advantages of our approach in the context of engineering complex quantum communication architectures.

2. An integrated cavity-waveguide spontaneous parametric downconversion source

For practical applications in quantum information and communication, having an integrated device [25–27] offers a number of advantages. For example, stabilizing a high-finesse doubly resonant cavity can prove challenging. In a monolithic design, such as the one provided by an integrated cavity-waveguide, only the temperature of a single component needs to be stabilized. It is also by changing the temperature that the device is phase-matched for a variety of wavelengths. Another advantage of integration is that very short cavity lengths can be achieved, allowing one to increase the free spectral range (FSR), which will be important for what follows.

The generic structure of the proposed device is shown in figure 1 and consists of a periodically poled lithium niobate (PPLN) crystal, in which a waveguide has been created [28–31]. Other materials, such as periodically poled potassium titanyl phosphate

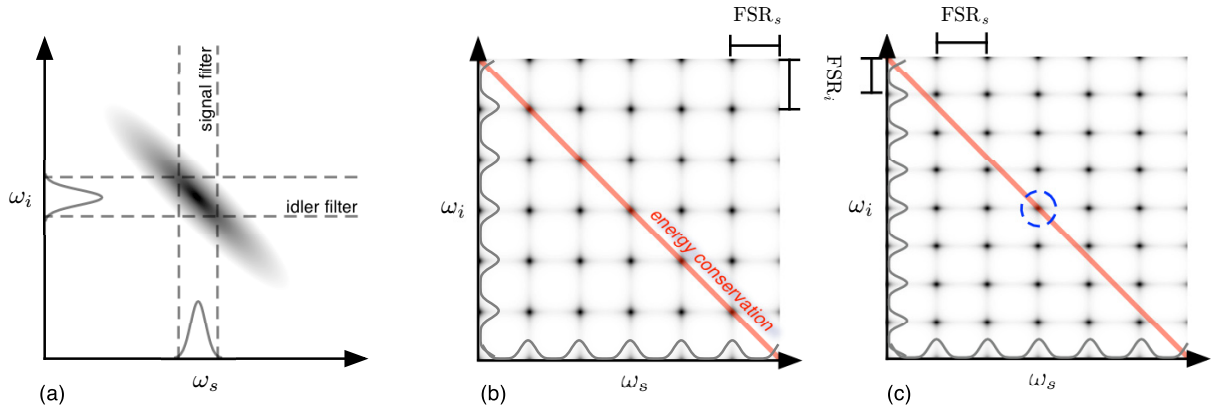

Figure 2. The joint frequency spectrum showing (a) typical correlations between the signal and the idler photon frequencies; (b) correlations in a doubly resonant SPDC source with no dispersion, where energy conservation (diagonal line) and resonance can be satisfied for a large number of adjacent cavity modes; and (c) correlations when the medium is dispersive: the spacing of signal and idler modes is different and fewer modes satisfy the cavity and energy conservation constraints (one is shown in the dashed circle).

(PPKTP) [32], can also be adopted. In an optimal device the entrance facet would be coated for high reflection at the signal and idler wavelengths, while the exit facet would have a reflectivity sufficient for achieving the desired finesse, but low enough to be the dominant loss mechanism.

We can treat this device as a Fabry–Perot cavity, whose finesse is completely determined by the losses and reflectivities:

$$\mathcal{F} = \frac{\pi}{2\arcsin\left(\frac{1-\rho^{1/2}}{2\rho^{1/4}}\right)}, \tag{1}$$

where ρ is related to the power in the cavity after a round trip and can be expressed as $\rho = R_1 R_2 10^{-2\alpha L/10}$, R_1 and R_2 are the reflectivities of the mirrors, α is the absorption coefficient expressed in dB cm^{-1}, L is the length of the crystal in cm and 2 accounts for the fact that the optical path per round trip is $2L$. In practice, the coating reflectivities R_1 and R_2 can be estimated by coating an optical blank with the same coating as the integrated device. Once the finesse of the cavity is measured, one can solve equation (1) for the waveguide loss coefficient α. In our initial test device [22], α was found to be 0.06 dB cm^{-1}. Having low internal losses is important, as these will ultimately limit the achievable finesse for a given cavity length.

2.1. Clustering in doubly resonant spontaneous parametric downconversion

The spectrum of photons generated by SPDC is usually determined by the phase-matching conditions between the pump, signal and idler fields in a nonlinear crystal [32], resulting in a typical joint frequency spectrum like that shown in figure 2(a). When the nonlinear crystal is placed inside a cavity [18–21], an extra set of constraints must be satisfied: photons can only be emitted in modes which are supported by the resonator. For a Fabry–Perot cavity the resonant modes are given by the Airy function. This second constraint on the joint frequency spectrum is represented in figure 2(b). When pumping with a narrow CW laser, energy conservation

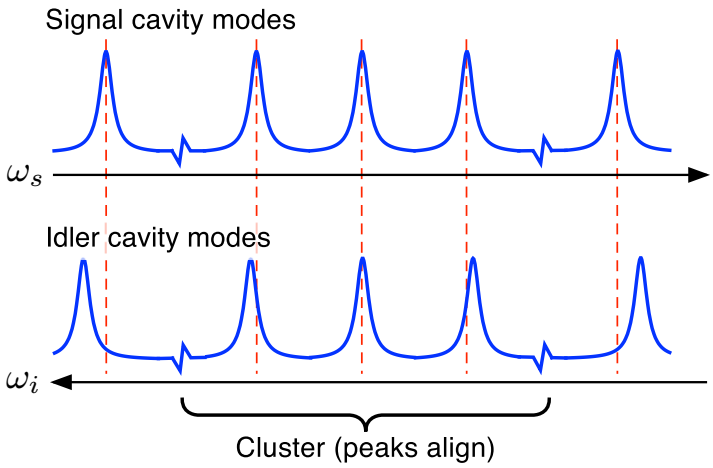

Figure 3. In a dispersive medium the optical length of a cavity varies with wavelength. SPDC occurs in such a cavity only when the double resonance condition is satisfied, i.e. when both signal and idler frequencies (satisfying $\omega_p = \omega_s + \omega_i$) are resonant.

($\omega_s + \omega_i = \omega_p$) will further restrict all photons to be emitted on the diagonal of the joint spectral function (figure 2(b)). If the refractive index is equal for both signal and idler photons, then the optical path length of the cavity, and the Airy functions, will be the same for both photons such that the distance between the peaks will be defined by the FSR of the cavity.

However, if the signal and idler photons have different dispersion characteristics, for example when they are non-degenerate in frequency or have distinct polarizations, the FSR at the signal and idler wavelengths will be different. In this situation, simultaneous resonance for both the signal and the idler arises only in regions of the spectrum where the peaks of the Fabry–Perot for the signal and the idler align (figures 2(c) and 3). These regions are called 'clusters' [33, 34], as they usually contain a number of emission peaks. However, as we shall see below, it is possible to design the finesse of the cavity, so as to produce clusters containing only a single peak.

2.2. Calculated and observed clustering spectra

The state of the photon pairs emitted by a doubly resonant OPO is given by [35]

$$|\Psi\rangle_{\mathrm{OPO}} = \int \mathrm{d}\omega_s \int \mathrm{d}\omega_i S(\omega_s, \omega_i) a_s^{\dagger}(\omega_s) a_i^{\dagger}(\omega_i) |vac\rangle, \tag{2}$$

where $S(\omega_s, \omega_i)$ is the joint spectral intensity,

$$S(\omega_s, \omega_i) = |f(\omega_s, \omega_i)|^2 \mathcal{A}_s(\omega_s) \mathcal{A}_i(\omega_i = \omega_p - \omega_s), \tag{3}$$

with the assumption of an infinite number of round trips of the photons inside the cavity. The quantity $f(\omega_s, \omega_i)$ represents the joint spectral amplitude in the absence of the cavity and, in the presence of a monochromatic pump, which is the case when the crystal is pumped in a CW mode, it reduces to the phase-matching function. $\mathcal{A}_j(\omega_j)$ are the Airy functions for the signal

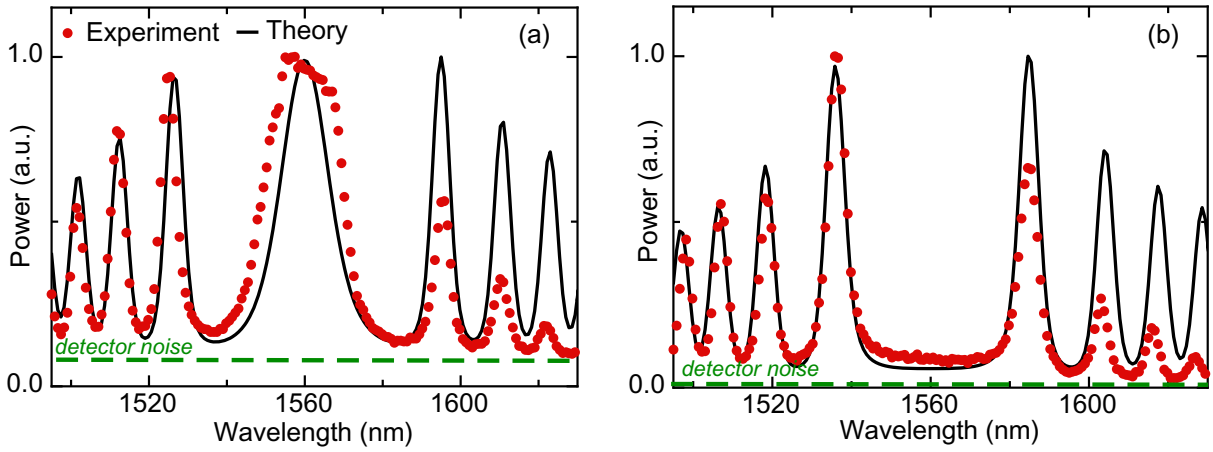

Figure 4. Measured (red dots) and calculated (black solid line) SPDC spectra for a PPLN waveguide at two different temperatures. The calculated curve results from the convolution of equation (2) with the spectral resolution of the monochromator (Gaussian, 4 nm FWHM) with detector noise added (dotted green line). The residual background is due to the overlap of the tails of the Gaussian shape of the monochromator with the peaks. The detector noise is different in the two figures as the signal-to-noise ratio varied between the two measurements. See the text for details.

and the idler photons, which, as functions of the wavelength, are expressed as

$$\mathcal{A}_j(\lambda_j) = \left[1 + \frac{4\sqrt{R_1 R_2}}{(1-\sqrt{R_1 R_2})^2}\sin^2(\phi_j)\right]^{-1}, \tag{4}$$

where $\phi_j = 2\pi L n_{\text{eff}}(\lambda_j)/\lambda_j$. Here n_{eff} is the wavelength-dependent effective refractive index inside the waveguide, taking into account the material and the waveguide dispersion.

To demonstrate that the clustering effect arises from the dispersion, we use the previous equations to reproduce the measured frequency spectra previously reported [22]. We consider a PPLN waveguide with length $L = 3.6$ cm, poling period $\Gamma = 16.6\,\mu$m, at a temperature $T = 128.6\,^{\circ}$C with mirror coating reflectivities of $R_1 = R_2 = 0.85$. For a pump at 780 nm, the phase matching is satisfied for the generation of photon pairs degenerate around 1560 nm. In this first instance, as we are interested only in the clustering effect; we can neglect the phase-matching condition, which is much larger than the effects we are studying. To model the emission spectrum we multiply the Airy function transmissions for the idler and the signal photons, whose frequencies are set by the energy conservation. The wavelength dependency of the extraordinary refractive index for the PPLN is given by the Sellmeier equation reported in [36], which have been adapted to take into account the waveguide dispersion.

Figure 4 shows the SPDC spectra emitted by this waveguide resonator for two different temperatures, as measured in [22] (red dots) and calculated (black solid line). The measurements were carried out by sending the SPDC photons through a monochromator and by detecting them with an InGaAs APD. The low resolution of the monochromator (4 nm full width at half maximum (FWHM)) averages over the fine structure within the clusters. As one moves away from the degeneracy point (central cluster) the clusters become narrow with respect to the monochromator's resolution, which results in an apparent reduction in their height. This effect

is well reproduced experimentally. The detector efficiency gradually decreases above 1560 nm so that the experimental peaks at higher wavelengths appear smaller than predicted by theory.

Our model is in good agreement with the measured data, with the clusters found at the same frequencies and the temperature difference between the configuration with (figure 4(a)) and without (figure 4(b)) the central cluster at 1560 nm is $\approx 0.07\,^{\circ}$C in the experiment and $0.08\,^{\circ}$C in the calculations. Furthermore, the model confirms its dependence on the finesse of the cavity, as observed in [22].

3. Designing a source of pure narrow-band photons with an integrated cavity-waveguide

Engineering a single-mode SPDC source via the clustering effect requires the clusters to be sufficiently narrow such that they can contain only one spectral mode of the cavity and that the FSR is sufficiently large so as to allow for low-loss filtering of the desired mode.

3.1. Determining the finesse

A cluster contains M modes when the difference between the spectral range corresponding to these modes for the idler and the same range for the signal is equal to the single-mode bandwidth. In quantitative terms, the number of modes within the cluster bandwidth can be expressed as

$$M(\mathrm{FSR_i} - \mathrm{FSR_s}) = \Delta\nu, \tag{5}$$

where $\mathrm{FSR_{i,s}}$ is the FSR for the idler and signal and $\Delta\nu$ is the mode bandwidth. We consider for $\Delta\nu$ the mean value of the idler and signal bandwidths:

$$\Delta\nu = \frac{\Delta\nu_\mathrm{i} + \Delta\nu_\mathrm{s}}{2} = \frac{\mathrm{FSR_i} + \mathrm{FSR_s}}{2\mathcal{F}}, \tag{6}$$

where $\mathcal{F}$ is the finesse of the cavity. In equation (6), $\mathcal{F}$ is assumed for simplicity to be the same for the idler and signal photons, implying that the mirrors' reflectivities and the internal losses of the waveguide resonator are independent of the wavelength. However, when this is not the case, similar calculations can be perfomed. Since $\mathrm{FSR_{i,s}} = c/(2N_{\mathrm{i,s}}L)$, where $N_{\mathrm{i,s}}$ is the group index at the idler and signal wavelengths, we can solve for the number of modes inside the cluster and determine the constraint on the finesse to have just a single mode:

$$M = \frac{1}{2\mathcal{F}}\left(\frac{N_\mathrm{s} + N_\mathrm{i}}{N_\mathrm{s} - N_\mathrm{i}}\right) \implies \mathcal{F}_{M=1} = \frac{1}{2}\left(\frac{N_\mathrm{s} + N_\mathrm{i}}{N_\mathrm{s} - N_\mathrm{i}}\right). \tag{7}$$

Therefore, finesse values larger than $\mathcal{F}_{M=1}$ are good to select single spectral modes. In figure 5, we give examples of the finesse $\mathcal{F}_{M=1}$, as a function of the signal wavelength, in the case of a 532 nm or a 780 nm pump. The different dispersions in the case of type 0 (eee) and type II (eoe) interactions for PPLN and PPKTP are considered. For the dispersion of the ordinary refractive index in PPLN and PPKTP, we use the Sellmeier equations reported in [37] and [38], respectively. For a certain signal wavelength, the idler is determined via energy conservation and then the dispersion at the two wavelengths is considered. The phase-matching condition for different wavelengths is not taken into account but can be defined for a variety of interactions with specific values of the poling period.

It is evident from these examples that, in the telecom regime, Type II PPLN and PPKTP crystals require lower values of the finesse, making the realization of integrated cavity-waveguides easier. For the type 0 interactions the required finesse becomes very high when

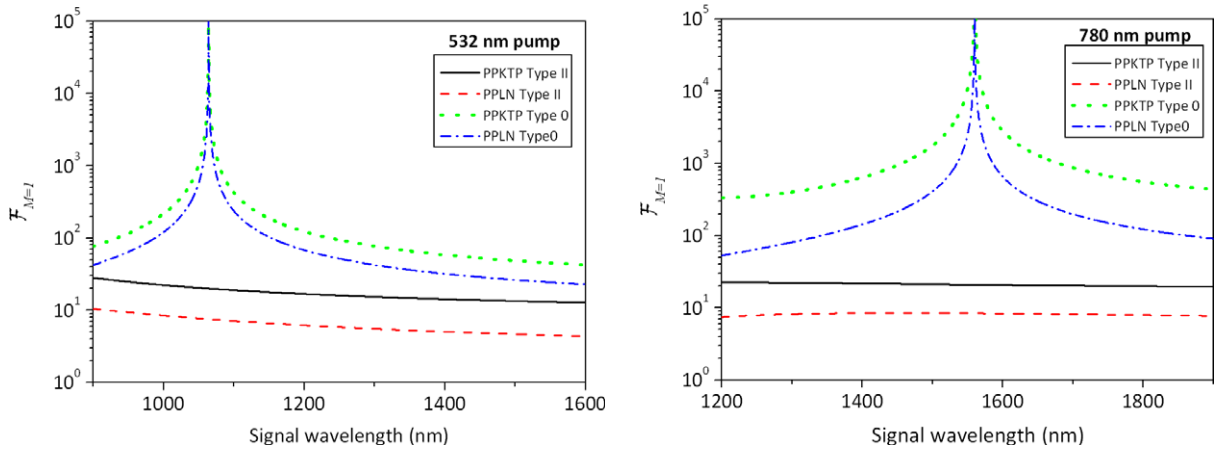

Figure 5. The finesse $\mathcal{F}_{M=1}$, corresponding to one mode in the clusters, for a 532 nm (left) and a 780 nm (right) pump, as a function of the signal wavelength. Type 0 (eee) and type II (eoe) interactions in PPKTP and PPLN are considered.

the signal wavelength is double the pump. In this configuration, the signal and idler have the same wavelength and undergo the same dispersion, increasing the finesse value according to equation (7).

Note that these considerations only provide a lower bound for the value of the finesse and, according to the needs, one has to define the length and the reflectivities of the mirrors of the cavity in order to have the desired mode bandwidth and internal losses.

3.2. Finding the optimal parameters of the integrated cavity-waveguide

In order to design a single-mode source with an integrated waveguide resonator with a precise value of the finesse, one has to know the absorption coefficient and optimize the values of R_2 and L to take into consideration the losses inside the crystal. Therefore, let us calculate the probability p_{out} of emitting photon pairs. With a reasoning similar to that in [22], assuming the initial generation of the photon pairs in the center of the waveguide, we find that

$$\begin{aligned} p_{\text{out}} &= 10^{-(\alpha/2)L/10}(1-R_2)\sum_{n=0}^{\infty}(R_1R_2 10^{-2\alpha L/10})^n \\ &= \frac{10^{-(\alpha/2)L/10}(1-R_2)}{1-R_1R_2 10^{-2\alpha L/10}}. \end{aligned} \tag{8}$$

The probability p_{out} depends on the length L of the cavity-waveguide. Clearly, for larger values of L the probability p_{out} decreases, although, to keep the finesse fixed, the reflectivity R_2 needs to be increased. Therefore, shorter crystals guarantee a small amount of overall loss and a large FSR, which is necessary for the efficient selection of a single spectral mode in the clusters.

3.3. Purity of the heralded photon state

This engineered photon pair source, in conjunction with sufficiently fast detectors, can be shown to produce heralded pure single photons. The clustering effect allows one to isolate a single spectral mode for the idler and the signal photon. Then, in order to achieve the spectro-temporal

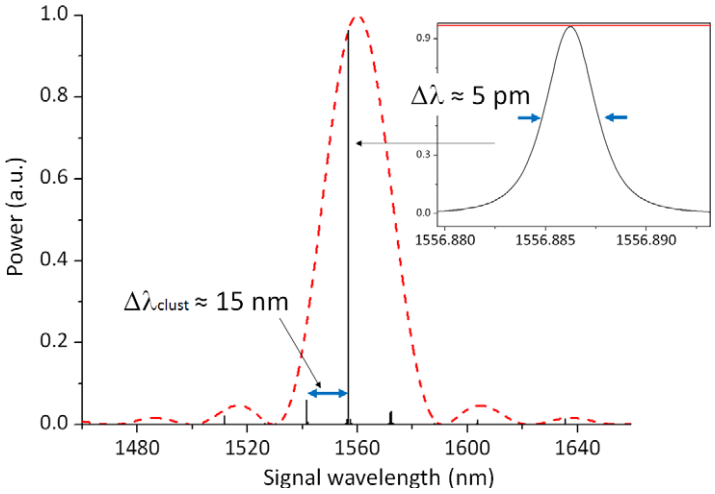

Figure 6. Frequency spectrum versus the signal wavelength, affected by the clustering effect, of an integrated cavity-waveguide whose parameters are indicated in the text. The red (dashed) line represents the phase-matching envelope. Right inset: zoom of the central single spectral mode.

purity of the heralded photon [16, 39], one has to adopt a detector on the heralding side with a resolution time τ_{res} smaller than the coherence time of the photon $\tau_c = 1/(\pi\,\Delta\nu)$ [18]. In [39], the condition $\Delta\nu \cdot \tau_{res} < 4$ has to be fulfilled in order to guarantee a single-mode measurement. Standard detectors, having a timing resolution of the order of hundreds of picoseconds, require $\Delta\nu \ll 1$ GHz, which is easily satisfied by this source.

Furthermore, the spatial purity of the heralded photon is guaranteed by coupling it into a single-mode optical fibre at the cost of some losses that depend on the emission properties of the source. However, single-mode waveguides have been shown to have very efficient (∼90%) coupling to single-mode fibers [31].

4. An optimized integrated cavity-waveguide source

Let us now consider a specific device design. A CW laser at 780 nm pumps a type II PPLN cavity-waveguide. From equation (7), we know that, in order to obtain a single-mode source at 1560 nm, we need a finesse larger than 10. Now, to have a sufficiently large FSR, we consider a crystal of length $L = 1$ mm. By assuming $R_1 \approx 1$ and $R_2 = 0.95$, which are attainable with current reflection coating technology, we obtain a finesse of 116.2 from equation (1). For the absorption coefficient we use the value of $\alpha = 0.06\,\mathrm{dB\,cm^{-1}}$, indicated in [22]. Using equation (8), we find a value for p_{out} of 95%.

By adopting the model described in section 2.2, we calculate the resonances of the cavity affected by the clustering effect at the temperature of $T = 80.14\,^{\circ}\mathrm{C}$. This is illustrated in figure 6, where the spectrum is reported with respect to the signal wavelength and the red (dashed) curve represents the phase-matching envelope, calculated using the model reported in [32]. The phase mismatch Δk can be expressed as $\Delta k = k_p - k_i - k_s - 2\pi/\Lambda$, where $k_{p,i,s}$ are the projection of the pump, idler and signal wave numbers to the direction of the waveguide and Λ is the effective poling period, which ensures phase matching.

As can be seen from figure 6, the spectrum is characterized by a series of resonances, which are inside distinct clusters. The phase-matching envelope contains only three single-mode clusters, which are present at a spectral distance of $\Delta\lambda_{\text{clust}} \approx 15$ nm: it is therefore possible to filter the central mode, for example, by simply using a prism or a notch filter, which have negligible transmission loss. This device represents an example of a single-mode SPDC cavity-waveguide which does not need additional, lossy, narrow-band filters and produces photons with a bandwidth of $\Delta\lambda = 4.6$ pm (right inset).

Let us now consider the purity of this system when used as a source of heralded single photons. A bandwidth of 4.6 pm ($\Delta\nu = 0.57$ GHz at 1560 nm) means that we need a detection timing resolution less than 7 ns to satisfy $\tau_{\text{res}} \cdot \Delta\nu < 4$ [39]. Standard InGaAs APDs (like the ID210, IDQuantique) typically have $\tau_{\text{res}} \approx 350$ ps. Therefore, heralded photons (with a high degree of purity) are achievable using quite straightforward and practical detection techniques.

In order to evaluate the brightness of the photon pairs generated by such a system, we take into account the measured brightness value reported in [40] for a 3 cm type II PPLN waveguide pumped by a CW laser at 777 nm and generating photons in a degenerate configuration at 1554 nm. The brightness of such a source is 6×10^2 photon pairs generated per second, per MHz of bandwidth and per mW of pump power. The brightness of a similar waveguide of 1 mm in a spectral window of $\Delta\lambda = 4.6$ pm would be 1.1×10^4 $(\text{s mW})^{-1}$. According to [18], double-resonant OPOs undergo an average enhancement factor per resonant mode equal to the square of the finesse $\mathcal{F}$ over π. Therefore, the optimized integrated cavity-waveguide reported in this subsection would have a brightness of 4.8×10^7 $(\text{s mW})^{-1}$ in the 4.6 pm single resonant mode shown in figure 6. In general, for applications in quantum communication, SPDC sources need to generate less than 0.1 photon pair per coherence time in order to limit the emission of double pairs. Since the coherence time of these photons is $\tau_{\text{c}} = \frac{1}{\pi\Delta\nu} = 560$ ps, the pump power necessary for emitting 0.1 photon pair per coherence time is about 4 mW. Therefore, the enhancement factor provided by the cavity allows one to use a low pump power.

5. Discussion

Engineering pure narrowband photon states that avoid the use of external filters is fundamental for performing a variety of quantum communication applications and complex multi-photon experiments. Because of the Gaussian loss induced by the filters, some protocols, such as device-independent QKD, simply cannot be implemented, since it becomes impossible to close the detection loophole. On the other hand, for the same Gaussian filtering factor, multiphoton experiments become extremely slow and practically unfeasible.

Figure 7 represents one of these most fundamental and important measurement schemes in quantum information science: the interference between two independent quantum systems. This configuration is commonly used, for example, to measure the Hong–Ou–Mandel interference between the photons γ_2 and γ_3, which are heralded by the detectors D_1 and D_4, respectively. Achieving unit interference visibility at beamsplitter B requires that the photons are in pure and indistinguishable states. Alternatively, by using the detectors D_2 and D_3 one can use this as a Bell state measurement (BSM) to herald a successful teleportation, as required for device-independent QKD [4], or entanglement swapping, as shown in [16]. We have shown that with this integrated OPO source, in conjunction with fast detection, one can efficiently herald pure

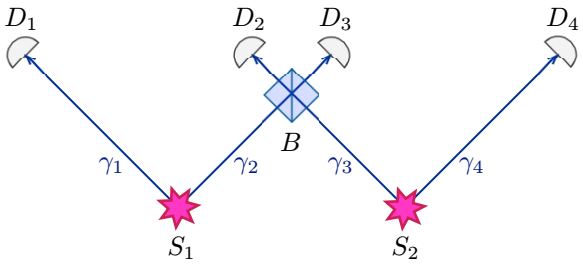

Figure 7. Photon interference scheme. The visibility of the Hong–Ou–Mandel interference of the photons γ_2 and γ_3, which are heralded by the detectors D_1 and D_4, respectively, is maximum when these two photons are in pure and indistinguishable states.

single photons. As such, the interference between the pure single photons produced by two such systems should be capable of a high degree of HOM interference.

In [16], a Hong–Ou–Mandel interference with waveguide-based sources followed by 10 pm external filters has been reported. If we were to replace the sources used in this experiment with two cavity-waveguides and, hence, to remove the lossy filtering system, we estimate an increase in the rate of such an experiment by almost two orders of magnitude, even before considering the improvements in fiber coupling and detector efficiencies achieved over the last few years. The visibility of the Hong–Ou–Mandel experiment in [16] was limited by multi-pair emission and by polarization fluctuations due to long integration times. The increased efficiency of this new approach would allow one to reduce the pump power, and hence the multi-pair emission rate, as well as reducing the integration times, thus significantly reducing the constraints on stabilization of the system. It is clear that this integrated solution, which is capable of exploiting standard detection schemes, provides significant advantages with respect to current approaches and is an important resource for future quantum networks.

6. Conclusions

We have outlined a model for the clustering effect in an integrated cavity-waveguide SPDC photon pair source pumped in a CW mode. We have shown how this effect can be engineered in order to emit narrow-band photons and to avoid the use of external filters. In conjunction with the fast detection of one photon of the generated pairs, one can efficiently herald pure narrow-band single photons. Due to the very narrow bandwidth of the photons, we expect that this will be of much interest, not only for quantum communication, but for a wide range of emerging quantum technologies and more fundamental investigations such as all-optical, loophole-free, Bell experiments.

Acknowledgments

We thank H Zbinden, N Sangouard, C Clausen and N Gisin for valuable discussions. This work was supported by the EU projects Qessence, QuReP and the Swiss NCCR-QSIT.

References

[1] Duan L M, Lukin M D, Cirac J I and Zoller P 2001 Long-distance quantum communication with atomic ensembles and linear optics *Nature* **414** 413

[2] Simon C, de Riedmatten H, Afzelius M, Sangouard N, Zbinden H and Gisin N 2007 Quantum repeaters with photon pair sources and multimode memories *Phys. Rev. Lett.* **98** 190503

[3] Sangouard N, Simon C, de Riedmatten H and Gisin N 2011 Quantum repeaters based on atomic ensembles and linear optics *Rev. Mod. Phys.* **83** 33

[4] Acín A, Brunner N, Gisin N, Massar S, Pironio S and Scarani V 2007 Device-independent security of quantum cryptography against collective attacks *Phys. Rev. Lett.* **98** 230501

[5] Dowling J P 2008 Quantum optical metrology—the lowdown on high-noon states *Contemp. Phys.* **49** 125

[6] Afek I, Ambar O and Silberberg Y 2010 High-noon states by mixing quantum and classical light *Science* **328** 879

[7] Knill E, Laflamme R and Milburn G J 2001 A scheme for efficient quantum computation with linear optics *Nature* **409** 46

[8] Raussendorf R and Briegel H J 2001 A one-way quantum computer *Phys. Rev. Lett.* **86** 5188

[9] Garay-Palmett K, McGuinness H J, Cohen O, Lundeen J S, Rangel-Rojo R, U'ren A B, Raymer M G, McKinstrie C J, Radic S and Walmsley I A 2007 Photon pair-state preparation with tailored spectral properties by spontaneous four-wave mixing in photonic-crystal fiber *Opt. Express* **15** 14870

[10] Brańczyk A M, Fedrizzi A, Stace T M, Ralph T C and White A G 2011 Engineered optical nonlinearity for quantum light sources *Opt. Express* **19** 55

[11] Söller C, Cohen O, Smith B, Walmsley I and Silberhorn C 2011 High-performance single-photon generation with commercial-grade optical fiber *Phys. Rev.* A **83** 031806

[12] Gisin N and Thew R 2007 Quantum communication *Nature Photonics* **1** 165

[13] Gisin N and Thew R T 2010 Quantum communication technology *Electr. Lett.* **46** 965

[14] Halder M, Beveratos A, Thew R T, Jorel C, Zbinden H and Gisin N 2008 High coherence photon pair source for quantum communication *New J. Phys.* **10** 023027

[15] Kwiat P G, Eberhard P H, Steinberg A M and Chiao R Y 1994 Proposal for a loophole-free Bell inequality experiment *Phys. Rev.* A **49** 3209

[16] Halder M, Beveratos A, Gisin N, Scarani V, Simon C and Zbinden H 2007 Entangling independent photons by time measurement *Nature Phys.* **3** 692

[17] Clausen C, Usmani I, Bussières F, Sangouard N, Afzelius M, de Riedmatten H and Gisin N 2011 Quantum storage of photonic entanglement in a crystal *Nature* **469** 508–11

[18] Lu Y J and Ou Z Y 2000 Optical parametric oscillator far below threshold: experiment versus theory *Phys. Rev.* A **62** 033804

[19] Wang H, Horikiri T and Kobayashi T 2004 Polarization-entangled mode-locked photons from cavity-enhanced spontaneous parametric down-conversion *Phys. Rev.* A **70** 043804

[20] Neergaard-Nielsen J S, Nielsen B M, Takahashi H, Vistnes A I and Polzik E S 2007 High purity bright single photon source *Opt. Express* **15** 7940

[21] Scholz M, Koch L, Ullmann R and Benson O 2009 Single-mode operation of a high-brightness narrow-band single-photon source *Appl. Phys. Lett.* **94** 201105

[22] Pomarico E, Sanguinetti B, Gisin N, Thew R, Zbinden H, Schreiber G, Thomas A and Sohler W 2009 Waveguide-based OPO source of entangled photon pairs *New J. Phys.* **11** 113042

[23] Korneev A *et al* 2004 Sensitivity and gigahertz counting performance of NbN superconducting single-photon detectors *Appl. Phys. Lett.* **84** 5338

[24] Thew R, Zbinden H and Gisin N 2008 Tunable upconversion photon detector *Appl. Phys. Lett.* **93** 071104

[25] O'Brien J L, Furusawa A and Vuckovic J 2009 Quantum communication *Nature Photonics* **3** 687

[26] Smith B J, Kundys D, Thomas-Peter N, Smith P G R and Walmsley I A 2009 Phase-controlled integrated photonic quantum circuits *Opt. Express* **17** 13516

[27] Sansoni L, Sciarrino F, Vallone G, Mataloni P, Crespi A, Ramponi R and Osellame R 2010 Polarization entangled state measurement on a chip *Phys. Rev. Lett.* **105** 200503

[28] Chou M H, Brener I, Fejer M M, Chaban E E and Christman S B 1998 1.5-μm-band wavelength conversion based on cascaded second-order nonlinearity in linbo3 waveguides *Photonics Technol. Lett.* **11** 653

[29] Tanzilli S, De Riedmatten H, Tittel H, Zbinden H, Baldi P, De Micheli M, Ostrowsky D B and Gisin N 2001 Highly efficient photon-pair source using periodically poled lithium niobate waveguide *Electr. Lett.* **37** 26

[30] Schreiber G, Hofmann D, Grundkötter W, Lee Y L, Suche H, Quiring V, Ricken R and Sohler W 2001 Nonlinear integrated optical frequency converters with periodically poled Ti:$LiNbO_3$ waveguides *Proc. SPIE* **4277** 144

[31] Roussev R V, Langrock C, Kurz J R and Fejer M M 2004 Periodically poled lithium niobate waveguide sum-frequency generator for efficient single-photon detection at communication wavelengths *Opt. Lett.* **29** 1518

[32] Fiorentino M, Spillane S M, Beausoleil R G, Roberts T D, Battle P and Munro M W 2007 Spontaneous parametric down-conversion in periodically poled KTP waveguides and bulk crystals *Opt. Express* **15** 7479

[33] Giordmaine J A and Miller R C 1966 Optical parametric oscillation in $LiNbO_3$ *Physics of Quantum Electronics* ed P L Kelley, B Lax and P E Tannenwald (New York: McGraw-Hill)

[34] Eckardt R C, Nabors C D, Kozlovsky W J and Byer R L 1991 Optical parametric oscillator frequency tuning and control *J. Opt. Soc. Am.* B **8** 646

[35] Jeronimo-Moreno Y, Rodriguez-Benavides S and U'Ren A B 2010 Theory of cavity-enhanced spontaneous parametric downconversion *Laser Phys.* **20** 1221

[36] Jundt D H 1997 Temperature-dependent Sellmeier equation for the index of refraction, n_e in congruent lithium niobate *Opt. Lett.* **22** 1553

[37] Edwards G J and Lawrence M 1984 A temperature-dependent dispersion equation for congruently grown lithium niobate *Opt. Quantum Electron.* **16** 373

[38] Bierlein J D and Vanherzeele H 1989 Potassium titanyl phosphate: properties and new applications *J. Opt. Soc. Am.* B **6** 622

[39] Huang Y P, Altepeter J B and Kumar P 2010 Heralding single photons without spectral factorability *Phys. Rev.* A **82** 043826

[40] Fujii G, Namekata N, Motoya1 M, Kurimura S and Inoue S 2007 Bright narrowband source of photon pairs at optical telecommunication wavelengths using a type-II periodically poled lithium niobate waveguide *Opt. Express* **15** 12769